Translational Oncology 15 (2022) 101299

Contents lists available at ScienceDirect

Translational Oncology

journal homepage: www.elsevier.com/locate/tranon

Original Research

EIF1A depletion restrains human pituitary adenoma progression

Rongxin Geng [1], Xiaonan Zhu [1], Xiang Tao, Junhui Liu, Haitao Xu [*]

Department of Neurosurgery, Renmin Hospital of Wuhan University, No. 238, Jiefang Road, Wuhan City, Hubei Province, China

ARTICLE INFO

Key words:
EIF1A
Pituitary adenoma
Cell proliferation
Cell migration
MAPK

ABSTRACT

EIF1A encodes a translation initiation factor in eukaryocyte and aberrant expression of EIF1A is deemed to be associated with dysfunctions in intracranial diseases. The goal of this research was to explore the impacts of EIF1A on progression of human pituitary adenoma (PA). We employed immunohistochemistry to assess the expression of EIF1A in PA and para-carcinoma tissues. After constructing EIF1A-knockdown cell models via lentivirus infection, we examined cell proliferation through CCK-8 assay and Celigo cell counting assay. Flow cytometry was utilized to detect cell apoptosis and the migration ability of experimental cells was estimated using wound-healing assay and Transwell assay. The activity of the apoptosis-related factor, Caspase 3, was also examined via Caspase 3 activity assay. Lastly, *in vivo* xenograft mouse models were established to verify findings derived from *in vitro* cell models. Our results affirmed upregulation of EIF1A in PA cells and revealed that depletion of EIF1A could seriously limit cell proliferation and weaken the capacity of cell migration, and also enhance apoptosis of tumor cells. Mechanistically, degradation in cell growth mediated by EIF1A knockdown may involve in activation of MAPK signaling but inactivation of PI3K/AKT signaling pathway. This study indicates EIF1A plays a prominent role in facilitating tumor cell proliferation and migration which may further contribute to PA progression.

Introduction

Pituitary adenoma (PA), the third most common intracranial tumor after glioma and meningioma, is known as originating from the pituitary gland and comprising more than 15% of all intracranial neoplasms [1]. As pituitary gland is the primary regulator of endocrinium, pituitary tumorigenesis could cause seriously hormonal imbalance, *e.g.*, hypersecretion of growth hormone (GH adenomas), prolactin (PRL adenomas) and adrenocorticotropin (ACTH adenomas), or possible loss of function (non-functioning adenomas) [2]. In spite of its benign nature, the growth of solid tumor is associated with considerable morbidity due to its oppressive injury to adjacent tissues, which gives rise to symptoms of nausea, headaches, dizziness or visual disturbances [3]. Patients with PA therefore suffer from an incremental risk of comorbidities and diminishing life quality. Thus, effective treatments should be as early as possible to minimize harmful effects [4]. Current clinical treatments for PA include surgical removal accompanied by pharmacological therapy, which could effectively alleviate the comorbidities and further prolong patients' survival [5]. Although the pathogenetic mechanisms underlying this disorder remain largely unknown, a previous study has suggested that epigenetic alterations or abnormities in activities of oncogenes and anti-oncogenes could be the possible triggers for PA [6].

EIF1A (eukaryotic translation initiation factor 1A X-linked), also known as *EIF1AX*, locates on human X chromosome (Xq22.12) and encodes an essential member of EIF-1A family which is a sequence family in relation to translation initiation [7]. The protein is 144 aa long and plays a role in stabilizing the combination of initiator Met-tRNA and the 40S ribosomal subunit [8]. In yeast (*Saccharomyces cerevisiae*), the corresponding gene encodes eIF1A, which functions as a highly-conserved translation initiation factor and is indispensable for yeast viability [9]. It has also been reported that eIF1A greatly contributes to cell proliferation and cell cycle in mice [10]. In human, the mutations of *EIF1A* gene were associated with progression of multiple cancer-related diseases, such as ovarian cancer [11], uveal melanomas, papillary thyroid carcinoma [12] and breast cancer. In patients with uveal melanomas, disomy for chromosome 3 is frequently involved in somatic mutations in gene *EIF1A* [13], which has been further proved that these mutations could increase discrimination against poor initiation sites in the process of transcription [14]. High expression level of EIF1A has been detected in breast cancer cells and can facilitate cell proliferation via targeting G1/S

* Corresponding author.
E-mail address: xuhaitaorenmin@163.com (H. Xu).
[1] These authors contributed equally to this work.

https://doi.org/10.1016/j.tranon.2021.101299
Received 18 June 2021; Received in revised form 25 November 2021; Accepted 25 November 2021

transition as well as suppressing p21 expression [15]. However, the potential role of EIF1A in intracranial tumor (*i.e.*, pituitary adenoma) has barely been investigated.

Herein, we detect the expression of EIF1A in PA cells and explore its potential role in tumor progression, aiming to disclosing the underlying EIF1A-mediated pathogenetic mechanism in this disease. Our findings unveil nonnegligible suppression in the capacity of cell growth and migration, but significant acceleration in cell apoptosis following depletion of EIF1A. *In vitro* experiments are subsequently verified through establishing mouse xenograft models. Mechanically, EIF1A may mediate PA progression via activating PI3K but deactivating MAPK signals which further exerts an influence on PA cell proliferation and apoptosis.

Materials and methods

Immunohistochemical staining

The slides of PA and para-carcinoma tissues were dewaxed in oven at 65 °C for half an hour and rinsed using ethanol for several times. In the subsequent process of EDTA antigen retrieval, slides were boiled for 30 min in the pressure cooker and then cooled down at room temperature, followed by 3% H_2O_2 treatment for blocking. The primary and secondary antibodies applied here were EIF1A (1:200, Cat. #bs-4314R, Bioss) and goat pAb rabbit IgG HRP (1:400, Cat. #ab97080, Abcam), after which we employed DAB and hematoxylin (Cat. #BA4041, Baso) to stain the slides. The slides were lastly observed and photographed under a microscope. The samples were from Renmin Hospital of Wuhan University and their collection and utilization have been approved with permission from all patients in accordance with the International Ethical Guidelines for Biomedical Research Involving Human Subjects prepared by CIOMS.

Establishment of lentiviral vector and shRNA transfection

Interfering RNAs were designed based on the human gene *EIF1A* and the target sequences were as follows, Human-EIF1A-1, 5′-ACGATTAGAAGCCATGTGTTT-3′; Human-EIF1A-2, 5′-CATCAGAGGGAAATTGAGAAA-3′ and Human-EIF1A-3, 5′-GTGTTCAAGGAGGATGGGCAA-3′. We thus constructed recombinant lentivirus vectors through cloning shRNAs into GFP (green fluorescent protein)-tagged linearized vectors (BR-V108, Shanghai Yibeirui Biomedical science and Technology Co., Ltd.) following the disposal of restriction endonucleases (Age I, Cat. #R3552L, NEB; EcoR I, Cat. #R3101L, NEB), and then transfected them into competent *E. coli* cells (Cat. #CB104-03, TIANGEN). Subsequently, we carried out qRT-PCR technique to detect the expression level of *EIF1A* mRNA and examine the positive clones. The primer sequences used in qRT-PCR were 5′-CCATGATTCCTTCATATTTGC-3′ (forward) and 5′-GAGCCGACACGGGTTAGGATC-3′ (reverse). Finally, the recombinant plasmids with target sequences were extracted (EndoFree Maxi Plasmid Kit, Cat. #DP118-2, TIANGEN) and transfected into experimental tumor cells.

Western blotting-based assay

The expression levels of the target protein, EIF1A, were examined in normal mouse pituitary epithelial cells (MPC) and mouse pituitary tumor cells (ATt-20 and GT1-1) using primary antibodies (EIF1A, 1:500, Rabbit, Cat. #bs-4314R, Bioss; GAPDH, 1:30000, Mouse, Cat. #60,004-1-Ig, Proteintech) and secondary antibodies (Goat anti-rabbit, 1:3000, Cat. # A0208, Beyotime; Goat anti-mouse, 1:3000, Cat. # A0216, Beyotime). Specifically, total protein was extracted using BCA protein assay kit (Cat. #23225, HyClone-Pierce). SDS-PAGE was prepared based on the molecular weight of a target protein and then exploited to separate proteins. After transferred onto a polyvinylidene difluoride membrane, proteins were blocked with TBST solution containing 5% skimmed milk on the membranes for 1 h at room temperature. The blotted membranes were thus incubated with primary antibodies and then the secondary antibody. Detailed information on primary antibodies and secondary antibodies when detecting the downstream proteins mediated by EIF1A in AtT-20 cells was shown in Table S1. Lastly, signals on the membranes were visualized using ECL-PLUS/Kit (Cat. #RPN2232, Amersham).

Cell proliferation assay

Proliferation of AtT-20 and GT1-1 cells were detected via CCK-8 assay and/or Celigo cell counting assay. For both AtT-20 and GT1-1 cells, we acquired cell suspension after trypsinization which was then added into each well (2000 cells/well) of the 96-well plate (Cat. #3596, Cornning). Then we appended 10 μL CCK-8 (Cat. #96992, Sigma) 2–4 h before termination of cell cultivation. Four hours later, we determined the absorption values at OD490 nm and finally got cell viability of the processed experimental cells. Furthermore, we additionally performed Celigo cell counting assay on GT1-1 cells. In brief, cell suspension was cultivated at 37 °C, 5% CO_2 overnight and cells were then counted with green fluorescence via Celigo assay for five consecutive days. Fold change was determined as follows, the multiple of cell proliferation in the shCtrl group divided by the multiple of cell proliferation in the shEIF1A group.

Flow cytometry

The examinations of cell cycle and cell apoptosis in AtT-20 and GT1-1 cell lines were performed via flow cytometry. Simply, the cells were firstly washed by PBS and digested by tyrisin, and then prepared after removing supernatant. In regard to the inspection of cell cycle, we subsequently fixed the cells via pre-cooled ethanol (70%, 4 °C) for more than 1 h. After the fixed liquid was dumped, cells were rewashed, centrifugated and then stained with 40 × PI solution (2 mg/mL; 100 × RNase, 10 mg/mL, 1 × PBS = 25:10:1000). As to cell apoptosis, cells were separately re-rinsed with PBS and binding buffer, and then stained using annexin V-APC (5 μL) in dark. Within 15 min, the percentage of cell apoptosis was evaluated using FACSCalibur (BD Biosciences).

Wound-healing assay

Wound-healing assay was performed in GT1-1 cells after the preparation of cell lysates. Experimental cells were cultured at 37 °C and 5% CO_2 overnight. Upon the end of cell cultivation, we used a 96-wounding replicator (Cat. #VP408FH, VP scientific) to scribe a straight line across the cell layer. Cells were then washed slightly for 2, 3 times and cultured for 24 h according to the extent of wound healing. Fluorescence micrographs were lastly taken and Cellomics (Cat. #ArrayScan VT1, Thermo) was used to analyze the migratory rate of GT1-1 cells.

Transwell assay

AtT-20 and GT1-1 cells were trypsinized and suspended in the serum-free medium, after which cell suspension was loaded into the Transwell room containing 30% FBS for incubation at 37 °C. After removing the culture medium, cells were fixed for 30 min and stained with 0.1% crystal violet for another 20 min. Then the cells were washed using PBS and lastly photographed under the microscope.

Caspase 3 activity assay

Changes of caspase 3 activity resulting from depleting EIF1A were examined in AtT-20 cells with a Caspase 3 activity assay kit (Cat. #BC3830, Beijing Solarbio Science & Technology Co., Ltd., China). Briefly, after centrifuged, experimental AtT-20 cells (2×10^4) were disposed using cell lysis solution and then placed on ice (4 °C) for 15

min. Subsequently, cells were centrifuged for 10–15 min (15,000 g) and the liquid supernatant was kept. Caspase 3 activity was represented by the absorption value using a Microplate reader at OD405 nm.

Xenograft model

The 4-week-old BALB/c nude female mice purchased from Beijing Vitalriver Experimental Animal Technology Co., Ltd were arbitrarily divided into two groups, and shEIF1A- and shCtrl-harboring AtT-20 cell suspensions (0.2 mL, 2×10^7 cells/mL) were then subcutaneously injected into these experimental animals of two groups, respectively. We measured the length and the width of the possible solid tumor, as well as the body weight of a given mouse model for the first time four days after injection. Then the measurements were performed every three days for another four times. After the last measurement, we disposed the experimental animals with 0.7% sodium pentobarbital (10 μL/g, SIGMA) and thus detected the extent of fluorescence expression using a Perkin Elmer (IVIS Spectrum). Subsequently, the mice were executed and the possible solid tumors were isolated for Ki67 pathological staining, in which we applied Ki67 (1:300, Cat. #ab16667, Abcam) and Goat Anti-Rabbit IgG H&L (1:400, Cat. #ab97080, Abcam) as the primary and the secondary antibody, respectively. The animal experiments were processed based on the protocol approved by Ethics committee of Renmin Hospital of Wuhan University (Issue NO., WDRM 20200520).

Statistics

For all statistical analysis in this research, a two-tailed $P < 0.05$ was

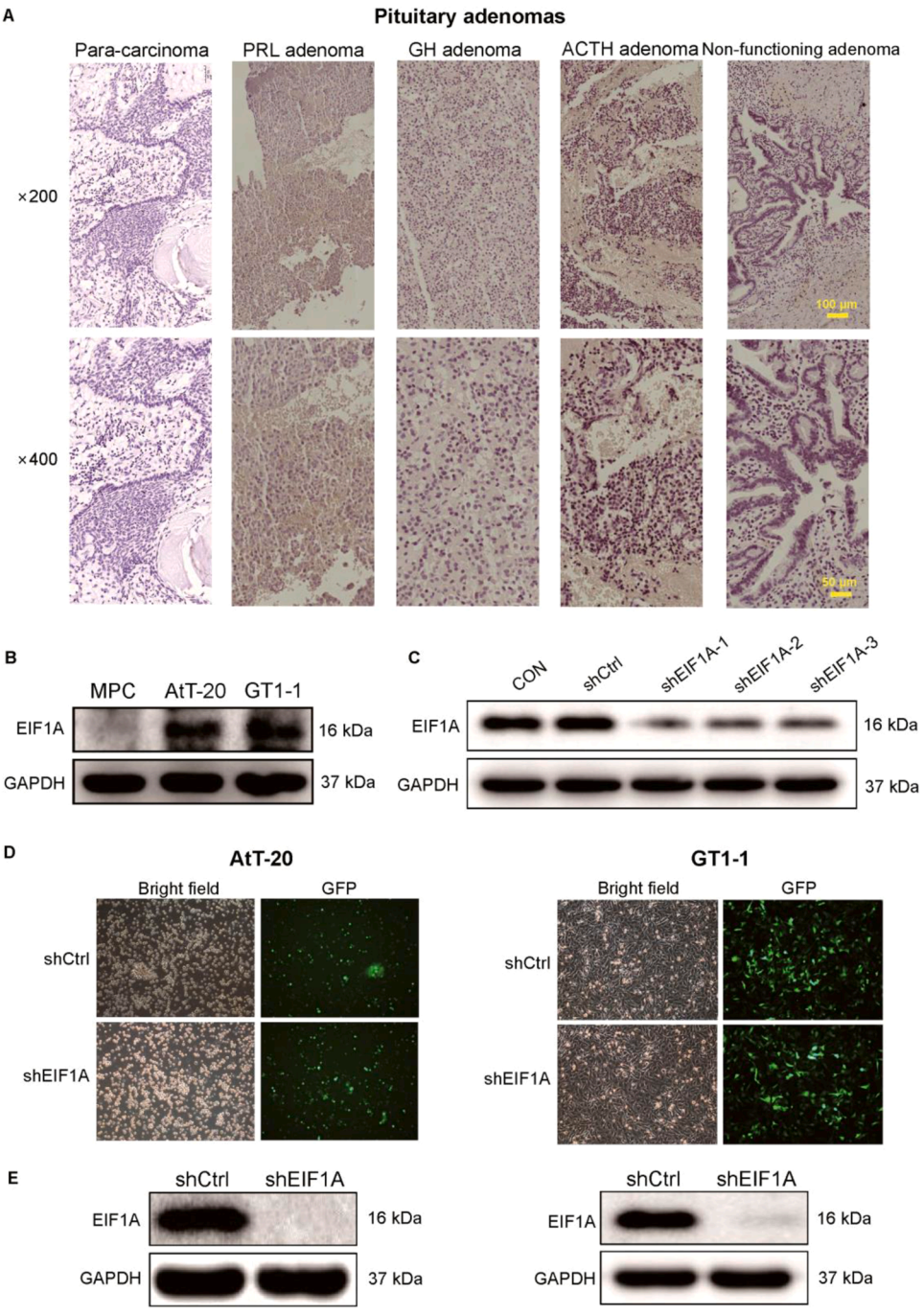

Fig. 1. The construction of EIF1A-silencing cell models *in vitro* via lentiviral transfection. (A) Immunohistochemistry staining for EIF1A expression in human pituitary adenomas (PA) and para-carcinoma tissue samples (× 200 and × 400). PRL, prolactin; GH, growth hormone; ACTH, adrenocorticotropin. **(B)** The level of EIF1A expression in MPC (normal mouse pituitary epithelial cells), AtT-20 and GT1-1 cells. **(C)** The comparison of EIF1A expression level between shEIF1A-transfected cells and negative controls in AtT-20 cells. **(D)** Fluorescence photomicrographs for the experimental cell groups in two cell lines (× 200) 72 h after lentivirus transfection. **(E)** The expression of EIF1A in both cell lines after transfected by shEIF1A- and shCtrl-harboring lentivirus, respectively. GAPDH, glyceraldehyde-3-phosphate dehydrogenase; GFP, green fluorescent protein.

considered as statistically significant. All cell experiments were conducted in triplicate and the data were shown as mean±SD. Student's *T* test was performed to compare the potential difference between two groups. SPSS 20.0 was utilized to run data analysis and plotting was achieved in GraphPad Prism 6.0.

Results

Constructing EIF1A-depletion cell models

Through immunohistochemistry staining, we firstly observed the expression of EIF1A in clinical PA and para-carcinoma tissue samples

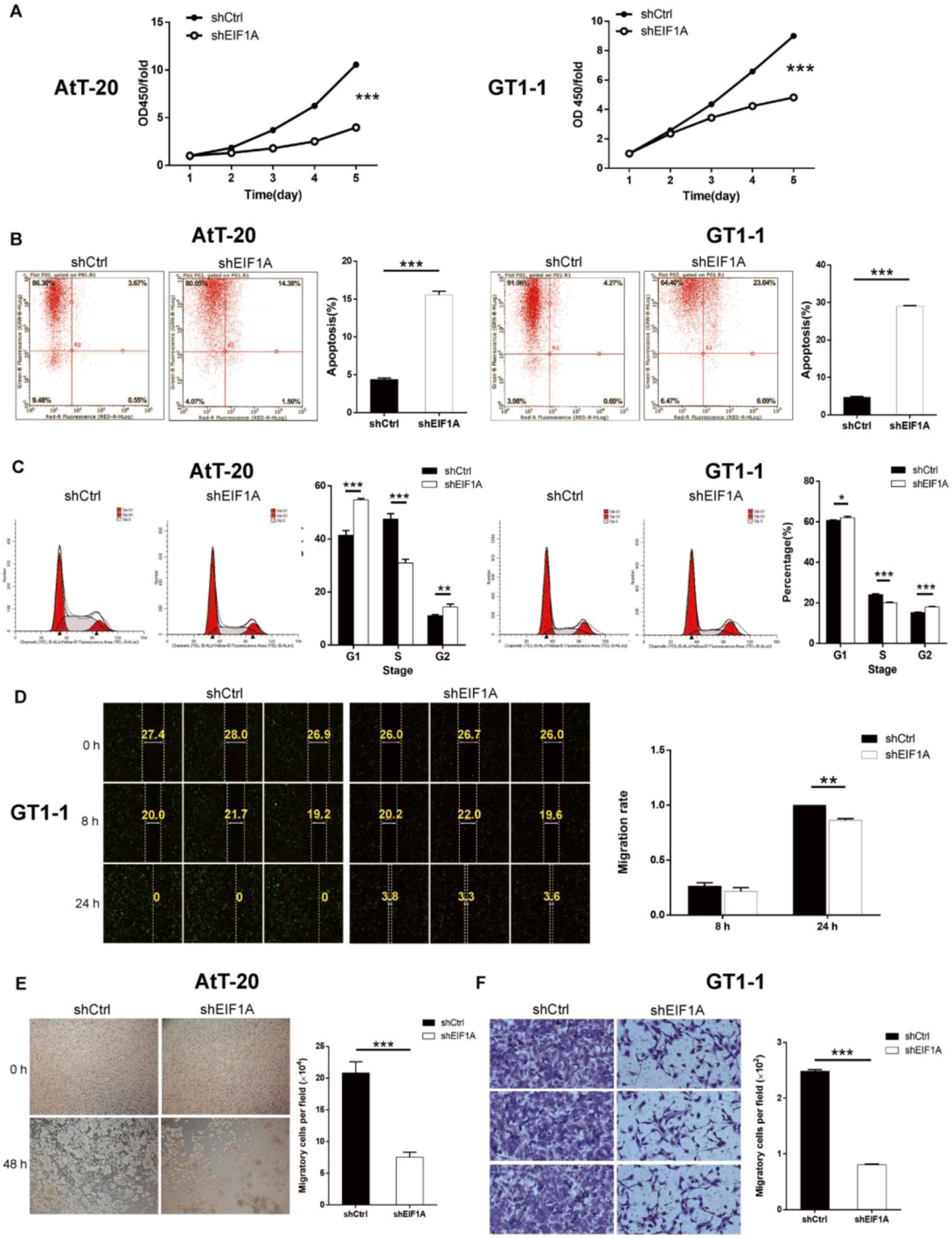

Fig. 2. EIF1A knockdown restrains proliferation, growth and migration of pituitary adenoma cells *in vitro*. (A) The comparison of absorptivity of AtT-20 cells and GT1-1 cells at wave length 450 nm through CCK-8 tetrazolium assay between shEIF1A and control groups. **(B)** The stained cells and percentages of cell apoptosis by flow cytometry in shEIF1A and shCtrl groups of AtT-20 and GT1-1 cell lines. **(C)** The percentages of cells in three cell-cycle phrases detected by flow cytometry in shEIF1A groups and controls of both cell lines. **(D)** Photographs from wound healing assay and the differences in the migration rate between shEIF1A-harboring cells and controls of GT1-1 cells. **(E)** Images of AtT-20 cells (× 200) by Transwell assay after lentiviral transfection for 24 h and the comparison test of migratory cell numbers between shEIF1A group and controls. **(F)** Images of GT1-1 cells (× 200) by Transwell assay after incubating for 16 h and the comparison test of migratory cell numbers between shEIF1A group and controls. Data are shown as Mean±SD. $^{*}P < 0.05$, $^{**}P < 0.01$, $^{***}P < 0.001$.

and the results indicated EIF1A was upregulated in several PA tissues compared with para-carcinoma tissues **(Fig. 1A)**. Then we detected the EIF1A level using WB assay and found higher EIF1A expression in both PA AtT-20 and GT1-1 cells than normal mouse pituitary epithelial cells (MPC) **(Fig. 1B)**. Before constructing EIF1A-knockdown PA cell models, we packaged three EIF1A-targeting shRNAs and transfected them into AtT-20 cells. Through WB assay, we selected the most effective one (shEIF1A-1) and utilized it for the following experiments **(Fig. 1C)**. The subsequent fluorescence photographing and WB assay demonstrated a pronounced decrease in EIF1A expression in both cell lines after silencing EIF1A with shRNA-harboring lentivirus **(Fig. 1D, E)**. We then exploited the successfully-constructed cell models with EIF1A depletion to launch the subsequent experiments.

EIF1A depletion impeded PA cell proliferation and migration in vitro

We then detected the effects of EIF1A depletion in both AtT-20 and GT1-1 cell lines on cell proliferation, apoptosis, cell cycle and cell migration. CCK-8 test showed that silencing EIF1A significantly lowered the number of viable cells in AtT-20 cell line ($P < 0.001$, fold change = -2.66) and GT1-1 cell line ($P < 0.001$, fold change = -1.9) in the first five consecutive days **(Fig. 2A-B)**. Similarly, a reduction of cell numbers in GT1-1 cells was also demonstrated by Celigo cell counting assay ($P < 0.01$, fold change = -1.54) **(Fig. S1)**. Compared with the negative controls, cell apoptosis resulting from flow cytometry was dramatically reinforced in the shEIF1A-harboring groups of both cell lines (AtT-20 cells, $P < 0.001$, fold change = 3.56; GT1-1 cells, $P < 0.001$, fold change = 6.13) **(Fig. 2B)**. As to cell cycle, the percentages of cells in G1 phrase after depleting EIF1A were significantly larger than controls (AtT-20 cells, $P < 0.001$; GT1-1 cells, $P < 0.05$), and it was the same case of the cells in G2 phrase (AtT-20 cells, $P < 0.01$; GT1-1 cells, $P < 0.001$). However, there was a pronounced decrease in the percentages of cells in S phrase following knocking down *EIF1A* in both cell lines (AtT-20 cells, $P < 0.001$; GT1-1 cells, $P < 0.001$) **(Fig. 2C)**, indicating that EIF1A regulated cell apoptosis through suspending cell mitosis in G1 phrase.

The subsequent wound-healing assay on GT1-1 cell line uncovered that transfection of shEIF1A led to a pronounced limitation on the cell migration rate after 24 h ($P< 0.01$) **(Fig. 2D)**. Similarly, migratory AtT-20 cells in the Transwell chambers were lessened after incubating for two days owing to EIF1A depletion ($P < 0.001$) **(Fig. 2E)**, with GT1-1 cells followed the same trend after incubating for 16 h ($P < 0.001$) **(Fig. 2F)**. To sum up, these outcomes clarified that dampening the expression of EIF1A could restrain PA cell proliferation and migration but accelerate cell apoptosis.

Molecular mechanism related to EIF1A in PA cells

Regarding the downstream proteins regulated by EIF1A in AtT-20 cells, the results of Caspase 3 activity assay kit indicated that Caspase 3 activity increased much more significantly following EIF1A depletion in the shEIF1A group than that in the shCtrl-harboring cells ($P < 0.001$) **(Fig. 3A)**. Other proteins related to cell apoptosis, MAPK and PI3K-AKT signaling pathways were then examined using WB assay. Specifically, downregulation of CCND1, CDK6, p-AKT and PIK3CA was found while GSK3β and MAPK9 were upregulated in EIF1A-silencing AtT-20 cells compared with shCtrl-harboring cells **(Fig. 3B)**. Apoptosis-related regulators, Bax and p53 levels were much higher in shEIF1A-harboring AtT-20 cells than controls, while Bcl-2 was downregulated as a result of EIF1A knockdown with shRNA lentivirus. **(Fig. 3C)**. Thus, we suggested that the involvement of PI3K/AKT and MAPK signaling pathways contributed to EIF1A-mediated tumor progression in AtT-20 cells.

Silencing EIF1A imposed restrictions on PA progression in vivo

After subcutaneously injecting AtT-20 cells into nude mice, we successfully constructed xenograft models and examined the consequence of cell transplantation. During the feeding period, the solid tumors of the experimental mice grew much slower in the shEIF1A group than controls, resulting in a much smaller tumor volume ($P < 0.05$) **(Fig. 4A)**. Five weeks after the injection, as a consequence of EIF1A knockdown, the total bioluminescent intensity of tumors in the shEIF1A group was significantly lower ($P < 0.05$) **(Fig. 4B)** than controls. Unsurprisingly, the solid tumors had a much lighter weight ($P < 0.01$) **(Fig. 4C)** than those isolated from control group. The following Ki67 staining on the isolated solid tumors affirmed downregulation of EIF1A in the shEIF1A group compared with negative controls **(Fig. 4D)**. The results above allowed us to demonstrate that EIF1A inactivation could effectively suppress *in vivo* PA tumor growth before the endpoint of the mouse experiment.

Discussion

The current study declares the vital role of EIF1A in PA progression. Specifically, we for the first time detect overexpression of EIF1A in PA glands. However, depleting *EIF1A* gene via lentiviral transfection substantially contributes to the weakened abilities of cell proliferation and migration in cell models, which are subsequently verified in xenograft mouse models. In the preliminary exploration of the underlying mechanisms, we disclose that downregulation of caspase-3 is responsible for the EIF1A-mediated retardation in cell apoptosis, while EIF1A accelerates cell survival via activating PI3K/AKT signaling but deactivating MAPK signaling pathways in pituitary tumor cells. The above-mentioned findings of our experiments assert EIF1A-mediated tumor progression in PA, which, to our knowledge, has not been reported before.

Mutations in *EIF1A* gene were generally associated with the incidence and progression of some disorders. For instance, The *EIF1A* gene is composed of NTT (N-terminal tail), RNA binding domain, Helical

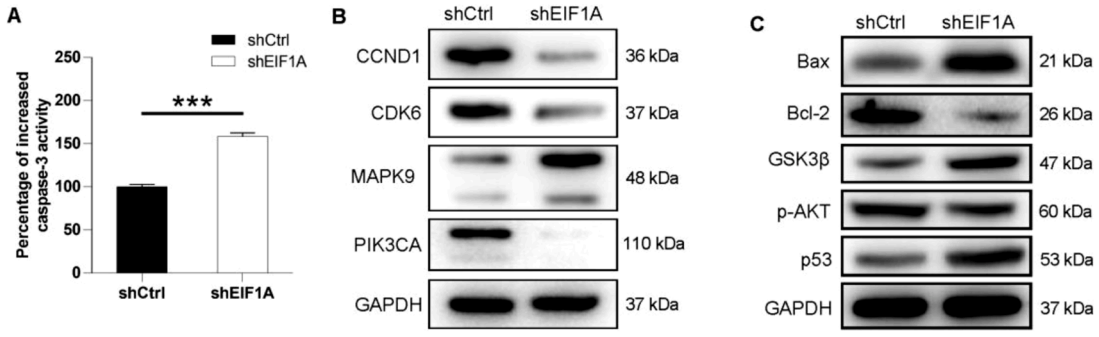

Fig. 3. Downstream signaling pathways associated with EIF1A activation. (A) Comparison of percentage of increased caspase 3 activity between shEIF1A and control groups in AtT-20 cells. **(B, C)** A western blot test on the protein levels associated with cell proliferation and apoptosis in AtT-20 cells. Data are shown as Mean±SD. ***$P < 0.001$.

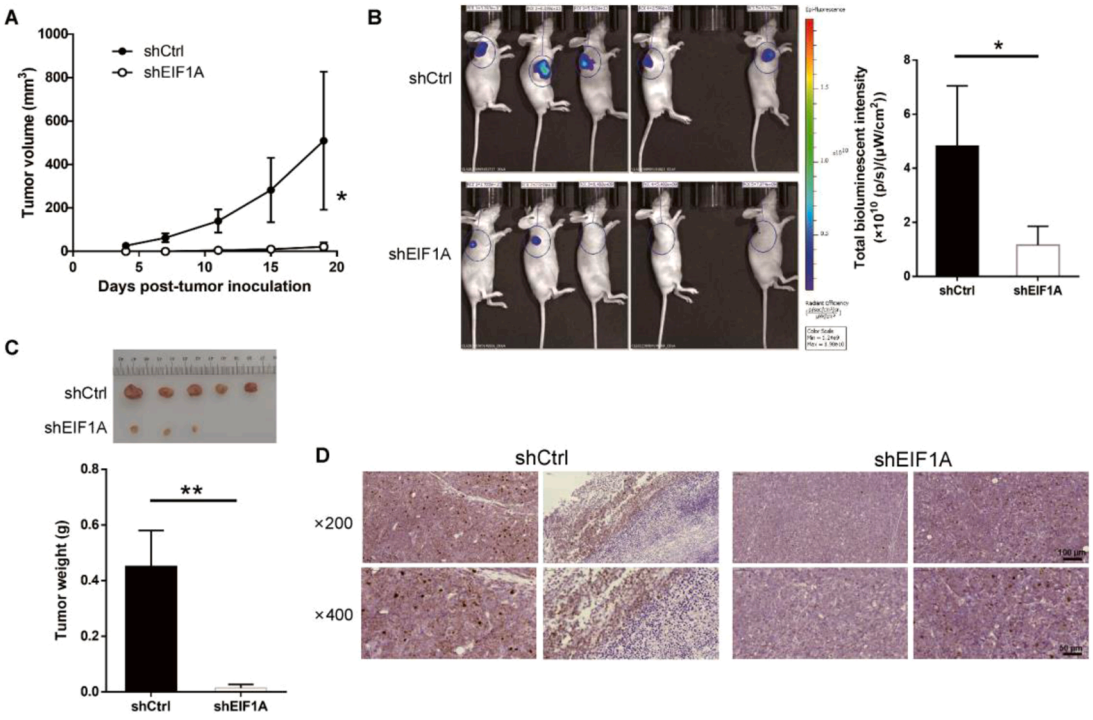

Fig. 4. EIF1A-mediated acceleration of tumor cell growth *in vivo*. **(A)** Tumor volumes after inoculated with experimental AtT-20 cells *in vivo* and the comparison between shEIF1A-harboring group and controls. **(B)** Bioluminescence photos and the comparison in the total bioluminescence intensity of the xenograft tumors (shEIF1A *vs.* shCtrl). **(C)** Extracted tumors from the mouse models and the comparison in tumor weight (shEIF1A *vs.* shCtrl). **(D)** Photomicrographs (× 200 and × 400) of the separated tumors in the experimental groups. Data are shown as Mean±SD. $^{*}P < 0.05$, $^{**}P < 0.01$.

domain and CTT (C-terminal tail) with most mutations occurring at the unstructured NTT in various tumor types [11]. In addition, mutations in *EIF1A* have also been described in patients with thyroid-affiliated diseases and different mutations were suggested to be relevant to different morbid phenotypes [16] and human racial groups [17]. Specifically, the splice site of intron5/exon 6 (A113_splice) on NTT of *EIF1A* is responsible for an ATF4-mediated dephosphorylation of EIF2α, which further enhances protein synthesis [18]. Variants on *EIF1A*-A113splice have been detected in thyroid carcinomas and benign nodules [19]. In the current study on PA, whether shEIF1A-mediated retardation in cell colony formation and reinforcement in cell apoptosis are due to variants on *EIF1A* in the genetic level remain unknown, which emphasizes the urgent need for deeper exploration of EIF1A in cancers.

As a critical participator during translation initiation, EIF1A may increase the transcriptional level and output in support of tumorigenesis. In light of our preliminary investigation on the underlying mechanisms in PA cells, we unfold the co-occurrence of CCND1 and CDK6 downregulation in shEIF1A-harboring AtT-20 cells, both of which act as essential proteins in cell cycle progression. CCND1 forms a complex with CDK6 as a regulatory subunit of which the activity is necessarily required for cell cycle G1 phase progression and G1/S transition [20]. In this case, EIF1A modulates cell proliferation in PA cells by targeting G1 phrase and promoting G1/S transition in the process of cell mitosis and dysregulation in EIF1A arrests cell cycle in G1 phrase, as shown in Fig. 2C. This finding is also in consistence with that in breast cancer cells [15]. We also unravel the EIF1A-mediated degradation in MAPK9, which is also known as c-Jun N-terminal kinase 2 (JNK2) and participates in various cellular processes in the MAPK signaling pathway. It abolishes the ubiquitination of p53, thus leads to p53 inactivation and protecting tumor cells from apoptosis [21]. In PA cells, EIF1A could take tumor-promoting actions by upregulating the pro-tumor factors, PIK3CA and p-AKT, as well as downregulating GSK3β in PI3K/AKT signaling pathway which is generally found active in many cancers [22]. Furthermore, the changes in expression of various apoptosis-related proteins, including caspase-3, Bax, Bcl-2 and p53, in the shEIF1A group are verified in cellular experiments. Specifically, caspase-3 is dramatically unregulated followed by the silence of *EIF1A* gene, indicating that EIF1A restrains PA cell apoptosis by principally inhibiting the activity of caspase-3. In addition, one of Bcl-2 associated proteins and apoptosis regulators, Bax, as well as p53 are considerably upregulated accompanied by the lowered expression of EIF1A. Downregulation of EIF1A also remarkably restrains the expression of Bcl-2, which is consistent with the results of cell apoptosis.

In short, through depleting EIF1A and building *in vitro* and *in vivo* models, we declare the prominent role EIF1A plays in PA progression which functions as a potent tumor promoter by enhancing PI3K/AKT signaling pathway but deactivating MAPK signaling pathway. The outcomes are conducive to the search and selection of the valuable therapeutic targets which are potentially effective for PA patients' treatment and improvement of the quality of their lives.

CRediT authorship contribution statement

Rongxin Geng: Investigation. **Xiaonan Zhu:** Writing – original draft. **Xiang Tao:** Writing – review & editing. **Junhui Liu:** Formal analysis. **Haitao Xu:** Formal analysis.

Declaration of Competing Interest

The authors declare no conflict of interest.

Acknowledgments

Not applicable.

Supplementary materials

Supplementary material associated with this article can be found, in

the online version, at doi:10.1016/j.tranon.2021.101299.

References

[1] S. Melmed, Mechanisms for pituitary tumorigenesis: the plastic pituitary, J. Clin. Invest. 112 (11) (2003) 1603–1618.

[2] S. Melmed, Pathogenesis of pituitary tumors, Nat. Rev. Endocrinol. 7 (5) (2011) 257–266.

[3] S.L. Asa, S. Ezzat, The pathogenesis of pituitary tumours, Nat. Rev. Cancer 2 (11) (2002) 836–849.

[4] T. Brue, F. Castinetti, The risks of overlooking the diagnosis of secreting pituitary adenomas, Orphanet J. Rare Dis. 11 (1) (2016) 135.

[5] S. Melmed, F.F. Casanueva, A. Klibanski, M.D. Bronstein, P. Chanson, S. W. Lamberts, et al., A consensus on the diagnosis and treatment of acromegaly complications, Pituitary 16 (3) (2013) 294–302.

[6] R. Yu, S. Melmed, Pathogenesis of pituitary tumors, Prog. Brain Res. 182 (2010) 207–227.

[7] H. Miyasaka, S. Endo, H. Shimizu, Eukaryotic translation initiation factor 1 (eIF1), the inspector of good AUG context for translation initiation, has an extremely bad AUG context, J. Biosci. Bioeng. 109 (6) (2010) 635–637.

[8] R. Spilka, C. Ernst, A.K. Mehta, J. Haybaeck, Eukaryotic translation initiation factors in cancer development and progression, Cancer Lett. 340 (1) (2013) 9–21.

[9] J.L. Battiste, T.V. Pestova, C.U. Hellen, G. Wagner, The eIF1A solution structure reveals a large RNA-binding surface important for scanning function, Mol. Cell 5 (1) (2000) 109–119.

[10] U. Sehrawat, F. Koning, S. Ashkenazi, G. Stelzer, D. Leshkowitz, R. Dikstein, Cancer-associated eukaryotic translation initiation factor 1A mutants impair Rps3 and Rps10 binding and enhance scanning of cell cycle genes, Mol. Cell. Biol. 39 (3) (2019).

[11] D. Etemadmoghadam, W.J. Azar, Y. Lei, T. Moujaber, D.W. Garsed, C.J. Kennedy, et al., EIF1AX and NRAS mutations co-occur and cooperate in low-grade serous ovarian carcinomas, Cancer Res. 77 (16) (2017) 4268–4278.

[12] N. Agrawal, R. Rehan, B. Arman Aksoy, B. Ally, H. Arachchi, S.L. Asa, J. Todd Auman, et al., Integrated genomic characterization of papillary thyroid carcinoma, Cell 159 (3) (2014) 676–690.

[13] M. Martin, L. Maßhöfer, P. Temming, S. Rahmann, C. Metz, N. Bornfeld, et al., Exome sequencing identifies recurrent somatic mutations in EIF1AX and SF3B1 in uveal melanoma with disomy 3, Nat. Genet. 45 (8) (2013) 933–936.

[14] P. Martin-Marcos, F. Zhou, C. Karunasiri, F. Zhang, J. Dong, J. Nanda, et al., eIF1A residues implicated in cancer stabilize translation preinitiation complexes and favor suboptimal initiation sites in yeast, Elife 6 (2017).

[15] Y. Li, L. Guo, S. Ying, G.H. Feng, Y. Zhang, Transcriptional repression of p21 by EIF1AX promotes the proliferation of breast cancer cells, Cell Prolif. 53 (10) (2020) e12903.

[16] A.S. Alzahrani, A.K. Murugan, E. Qasem, M.M. Alswailem, B. AlGhamdi, Y. Moria, et al., Absence of EIF1AX, PPM1D, and CHEK2 mutations reported in thyroid cancer genome atlas (TCGA) in a large series of thyroid cancer, Endocrine 63 (1) (2019) 94–100.

[17] J. Simões-Pereira, M.M. Moura, I.J. Marques, M. Rito, R.A. Cabrera, V. Leite, et al., The role of EIF1AX in thyroid cancer tumourigenesis and progression, J. Endocrinol. Invest. 42 (3) (2019) 313–318.

[18] G.P. Krishnamoorthy, N.R. Davidson, S.D. Leach, Z. Zhao, S.W. Lowe, G. Lee, et al., EIF1AX and RAS mutations cooperate to drive thyroid tumorigenesis through ATF4 and c-MYC, Cancer Discov. 9 (2) (2019) 264–281.

[19] A. Karunamurthy, F. Panebianco, S. JH, J. Vorhauer, M.N. Nikiforova, S. Chiosea, et al., Prevalence and phenotypic correlations of EIF1AX mutations in thyroid nodules, Endocr. Relat. Cancer 23 (4) (2016) 295–301.

[20] M. Malumbres, R. Sotillo, D. Santamaría, J. Galán, A. Cerezo, S. Ortega, et al., Mammalian cells cycle without the D-type cyclin-dependent kinases Cdk4 and Cdk6, Cell 118 (4) (2004) 493–504.

[21] N.V. Oleinik, N.I. Krupenko, S.A. Krupenko, Cooperation between JNK1 and JNK2 in activation of p53 apoptotic pathway, Oncogene 26 (51) (2007) 7222–7230.

[22] C. Bartholomeusz, A.M. Gonzalez-Angulo, Targeting the PI3K signaling pathway in cancer therapy, Expert Opin. Ther. Targets 16 (1) (2012) 121–130.